Inorganic Chemistry

Forum Article

pubs.acs.org/IC

Efficient Photocatalysts for CO_2 Reduction

Go Sahara[†] and Osamu Ishitani*[,†,‡]

[†]Department of Chemistry, Graduate School of Science and Engineering, Tokyo Institute of Technology, 2-12-1-NE-1, Ookayama, Meguro-ku, Tokyo 152-8550, Japan

[‡]CREST, Japan Science and Technology Agency, 4-1-8 Honcho, Kawaguchi-shi, Saitama 322-0012, Japan

ABSTRACT: Three types of photocatalytic systems for CO_2 reduction, which were recently developed in our group, are reviewed. First, two-component systems containing different rhenium(I) complexes having different roles; i.e., redox photosensitizer and catalyst in the reaction solution are described. The mixed system of a ring-shaped rhenium(I) trinuclear complex and *fac*-$[Re(bpy)(CO)_3(MeCN)]^+$ is currently the most efficient photocatalytic system for CO_2 reduction (Φ_{CO} = 0.82 at λ_{ex} = 436 nm). The second is a series of supramolecular photocatalysts, which have units with different functions in one molecule, i.e., redox photosensitizer, catalyst, and bridging ligand. The highest durability and speed of photocatalysis were achieved by using this system (Φ_{CO} = 0.45, TON_{CO} = 3029, and TOF_{CO} = 35.7 min^{-1}). The third is a novel type of artificial Z-Scheme photocatalyst for CO_2 reduction, of which photocatalysis is revealed by stepwise excitation of both a semiconductor photocatalyst unit and the supramolecular photocatalyst unit. This system has both strong oxidation and reduction powers.

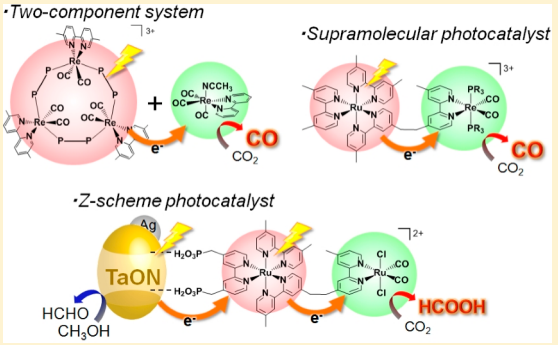

INTRODUCTION

Human beings are facing three serious problems that are related to each other, i.e., shortage of energy sources, shortage of carbon resources, and global warming.[1,2] In the biosphere, CO_2 is the main carbon source that is reductively converted to energy-rich carbohydrates by using solar light as the energy source and water as the reductant. However, we do not have such practical technologies and have been consuming much of the fossil resources, which were produced by photosynthesis and have then been stored under ground as both chemical and energy resources. Most of them have finally been burned, thus releasing a tremendous amount of CO_2 into the atmosphere. For solving these serious problems simultaneously, artificial photosynthesis systems, which can convert CO_2 to useful and energy-rich compounds using solar light as the energy source and water as the reductant, are probably the most ideal solution[3,4] (Scheme 1).

Scheme 2 illustrates the minimum functional requirements of artificial photosynthesis systems: the light-harvesting function for molecular photocatalysts due to the photon flux of sun light being very dilute and the small molecular size; both strong reduction and oxidation powers produced using relatively low-energy light, i.e., visible light, which should be achieved through a stepwise two-photon absorption system, the so-called artificial Z-Scheme; the water-oxidation catalyst; a catalyst for CO_2 reduction.

In this study, the photocatalysts for CO_2 reduction, which have been recently developed in our groups, are reported as some key technologies for developing such artificial photosynthesis systems. These are divided into three parts: two-component systems, supramolecular photocatalysts, and hybrids of the supramolecular photocatalyst with a semiconductor photocatalyst.

Scheme 1. Natural and Artificial Photosynthesis

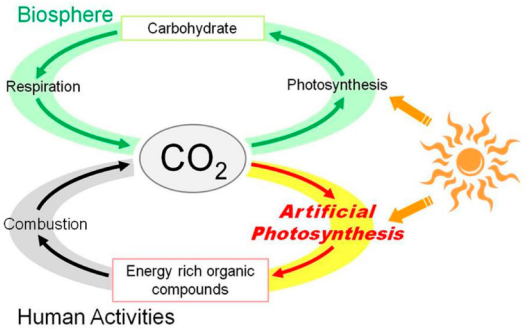

Molecular photocatalytic systems for CO_2 reduction have a dilemma to be solved; that is, in cases where the photochemical electron-transfer process is used, excitation by one photon usually induces only one-electron transfer but not multielectron transfer; however, one-electron reduction of CO_2 requires a highly negative potential (E° = −1.9 V vs NHE at pH = 7), and the product $CO_2^{\bullet-}$ is so active that controlling the selective product is difficult (eq 1).[5,6]

$$CO_2 + e^- \rightarrow CO_2^{\bullet-} \qquad E^\circ = -1.9\ V \tag{1}$$

Special Issue: Small Molecule Activation: From Biological Principles to Energy Applications

Received: November 6, 2014
Published: January 28, 2015

DOI: 10.1021/ic502675a
Inorg. Chem. 2015, 54, 5096−5104

Scheme 2. Requirements for a "Practical" Artificial Photosynthesis System

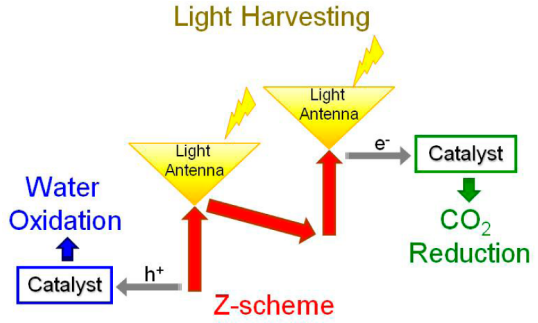

To solve this problem, two-component photocatalytic systems constructed with a redox photosensitizer that photochemically mediates one-electron transfer and a catalyst that converts one-electron transfer to multielectron reduction of CO_2 have been developed. Multielectron reduction of CO_2 drastically reduces the reduction potential of CO_2 and produces stable and useful products, e.g., CO and HCOOH (eqs 2 and 3).

$$CO_2 + 2H^+ + 2e^- \rightarrow HCOOH \qquad E^\circ = -0.61\ V \quad (2)$$

$$CO_2 + 2H^+ + 2e^- \rightarrow CO + H_2O \qquad E^\circ = -0.53\ V \quad (3)$$

RHENIUM(I) PHOTOCATALYSTS: TWO-COMPONENT SYSTEMS

Rhenium(I) complexes are now investigated widely as a photocatalyst and an electrocatalyst for CO_2 reduction.[7−10] In 1983, Lehn et al. reported the first photocatalytic system for CO_2 reduction using a rhenium(I) complex, i.e., *fac*-Re(bpy)-$(CO)_3L$ (bpy = 2,2′-bipyridine; L = Cl^- or Br^-) in a triethanolamine (TEOA) and *N*,*N*-dimethylformamide (DMF) mixed solution.[11,12] This system has attracted tremendous attention because of its high selectivity of CO formation and high efficiency (Φ_{CO} = 0.14; X = Cl^-). Although there were some studies reporting the photochemical reduction of CO_2 mainly using semiconductor photocatalysts before Lehn et al.'s report, the efficiency and selectivity of CO formation were much lower because of the more advantageous H_2 formation. Despite the unique and outstanding properties of rhenium(I) complexes as photocatalysts for CO_2 reduction, there were some serious defects: low durability of the photocatalyst (turnover number TON_{CO} = 27; X = Cl^-), slow speed of CO formation, and low absorption in the visible region [the rhenium(I) complexes are yellow].

Just after Lehn et al.'s report, some mechanistic investigations using laser flash photolysis techniques were reported by the different groups.[13−15] Both of them clearly showed that the lowest excited state of the rhenium(I) complex, which is a triplet metal-to-ligand-charge-transfer (^{3}MLCT) state, is reductively quenched by TEOA but not oxidatively quenched by CO_2. The reductive quenching gives the corresponding one-electron-reduced species (OERS) of the rhenium(I) complex. Loss of the Cl^- ligand from the OERS requires several seconds, and this slow process gives the so-called "17-electron species". Fujita and co-workers reported that, although reduced and coordinatively unsaturated [Re(4,4′-Me_2bpy)$(CO)_3$] can react with CO_2, this process is very slow [$k_{obs} \approx 0.003\ s^{-1}$ under ∼0.8 atm of CO_2 in tetrahydrofuran (THF)] because the added electron is mainly localized in the bpy ligand; i.e., Re^I(4,4′-$Me_2bpy^{\bullet-}$)$(CO)_3$ should have a more feasible electronic structure rather than Re^0(4,4′-Me_2bpy)$(CO)_3$.[16] The author supposed that this might be one of the reasons why the photocatalytic reduction using the rhenium(I) complexes is slow.

We investigated the effects of an anionic ligand in rhenium(I) complexes on the photocatalytic abilities for CO_2 reduction using *fac*-Re(bpy)$(CO)_3$X (X = Cl^-, SCN^-, and CN^-).[17] These complexes have similar photophysical and electrochemical properties (Table 1). However, the photocatalytic abilities of these complexes were drastically different: the photocatalytic ability of the complex with the SCN^- ligand was higher (Φ_{CO} = 0.20 and TON_{CO} = 30) than that of the Cl^- complex, whereas the CN^- complex did not show any photocatalytic activity for CO_2 reduction. On the basis of the investigation of the accumulation and reactivity of the OERS of the rhenium(I) complexes, we found that the OERS of the rhenium(I) complexes have two crucial roles: one as the precursor of the "17-electron species" produced by loss of the anionic ligand and the other as a second electron source for the "CO_2 adduct", whose structure is the subject of controversies (Scheme 3).

Table 1. Photophysical and Electrochemical Properties of *fac*-Re(bpy)$(CO)_3$X from References 14 and 17

X	λ_{max},[a] nm	λ_{em},[b] nm	Φ_{em},[b] %	τ,[b] ns	$E_{red}^{1/2}$,[c] V
Cl^-	384	637	0.003	25[d]	−1.67
SCN^-	396	635	0.003	30	−1.61
CN^-	374	611	0.013	87	−1.67

[a]In CH_2Cl_2. [b]In DMF. [c]Versus $Ag/AgNO_3$ in MeCN. [d]In MeCN.

Scheme 3. Photocatalytic Reaction Mechanism by *fac*-Re(bpy)$(CO)_3$NCS[17]

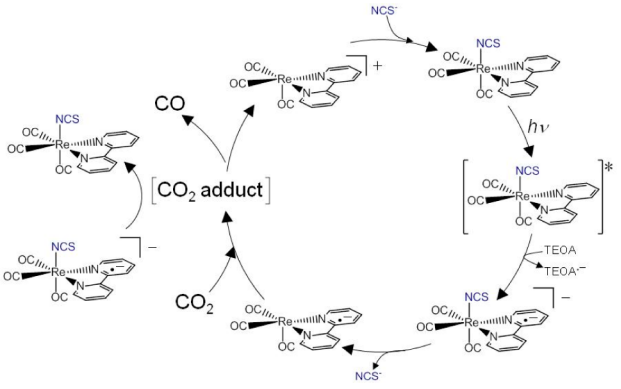

In the case of the CN^- complex, loss of the CN^- ligand from the OERS did not proceed at all; therefore, the CN^- complex could not work as a photocatalyst for CO_2 reduction. The stability of the OERS of the SCN^- complex was higher than that of the Cl^- complex. This should advantageously work as the source of the second electron even though it might be disadvantageous for the precursor of the "CO_2 adduct". Therefore, the OERS of the SCN^- complex should have a better balance than the Cl^- complex in the photocatalytic reduction of CO_2 between being the electron source and the precursor of the "CO_2 adduct". We recently found that

DOI: 10.1021/ic502675a
Inorg. Chem. 2015, 54, 5096−5104

$Re(bpy)(CO)_3(OCOOC_2H_4NR_2)$ (R = C_2H_4OH) formed in the reaction solutions of the various photocatalytic systems with the rhenium(I) complexes.[18] This complex should participate in the photocatalytic reactions as described above. Investigation of the roles of the CO_2 adduct in the photocatalytic reactions is in progress. The investigation on the accumulation of the OERS gave us insight for constructing a better photocatalytic system for CO_2 reduction using rhenium(I) complexes: there should be a limitation of photocatalysis if we use only one rhenium(I) complex because its OERS required two directly opposite properties, i.e., *instability* for giving the "CO_2 adduct" and *stability* for working as the electron donor. To overcome this conflict, we developed two-component systems containing different rhenium(I) complexes having different roles in the reaction solution. First, we chose *fac*-$[Re\{4,4'\text{-}(MeO)_2bpy\}(CO)_3\{P(OEt)_3\}]^+$ as the redox photosensitizer initiating the photochemical electron transfer because the OERS of this complex has high durability because of the high π-accepting ability of the $P(OEt)_3$ ligand and strong reduction power due to the electron-donating methoxy groups in the bpy ligand. *fac*-$[Re(bpy)(CO)_3(MeCN)]^+$ was used as the catalyst for CO_2 reduction because of the weak bonding ability of the acetonitrile (MeCN) ligand. The photocatalytic system containing the redox photosensitizer and catalyst in a ratio of 25:1 showed much higher efficiency in CO_2 reduction than the single-component systems: Φ_{CO} was 0.59 with irradiation at λ_{ex} = 365 nm.[17] Recently, we also developed a more efficient photocatalytic system using a ring-shaped rhenium(I) trinuclear complex (Chart 1), of which the Re units are connected with

Chart 1. Structure of the Ring-Shaped Rhenium(I) Trinuclear Complex[19]

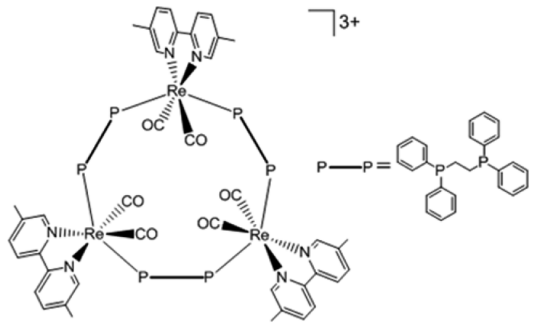

bidentate phosphine ligands, as the redox photosensitizer with the same catalyst. The rhenium ring has several outstanding properties as a redox photosensitizer, i.e., relatively strong absorption in the visible region, long lifetime of the excited state (τ_{em} = 5.4 μs), and high stability of the OERS, which are caused by the unique $\pi-\pi$ interaction between the diimine and the phenyl groups of the phosphine ligands. To the best of our knowledge, the mixed system of the rhenium ring and the MeCN complex exhibits the highest quantum efficiency for CO_2 reduction (Φ_{CO} = 0.82 at λ_{ex} = 436 nm and TON_{CO} = 526).[19]

SUPRAMOLECULAR PHOTOCATALYSTS

The two-component systems require collision between the OERS of the photosensitizer and the catalyst as one of the important processes in the overall photocatalytic reaction. This may become a rate-limiting process of the photocatalytic reaction. To avoid this, an excessive amount of the redox photosensitizer compared to the catalyst was sometimes added to the reaction solution in many reported two-component photocatalytic systems, which lowered $TON_{product}$ based on the photosensitizer used.[20,21] Furthermore, the two-component systems expose a serious concern in the cases where both photosensitizer and catalyst are immobilized on the surface of solid matter such as semiconductors and electrodes because the immobility of the photosensitizer and catalyst molecules in separated places makes the necessary collision very difficult. To overcome these problems, we tried to connect a redox photosensitizer and a catalyst for CO_2 reduction using a bridging ligand. This type of assembly is called a supramolecular photocatalyst, which has units with different functions in one molecule, i.e., redox photosensitizer, catalyst, and bridging ligand. Although this idea was not new, to the best of our knowledge, there had been no report of "good" supramolecular photocatalysts for CO_2 reduction; i.e., $TON_{product}$ of the supramolecular photocatalysts was lower than those of the corresponding mixtures of the corresponding mononuclear metal complexes and/or $TON_{product}$ was less than 1[22−24] before we reported the first highly efficient supramolecular photocatalyst.[25]

To formulate the molecular architecture of the supramolecular photocatalysts with high efficiency, durability, and speed, we first chose a tris(diimine)ruthenium(II)-type photosensitizer, which has a wide range of absorption bands in the visible region up to 560 nm, and the *fac*-Re(N^N)$(CO)_3$Cl-type complex as a catalyst unit, which absorbs only at wavelengths shorter than 450 nm; therefore, selective excitation of the photosensitizer unit is possible. Both the ruthenium photosensitizer and the rhenium catalyst were connected with various bridging ligands (Chart 2), and their photocatalytic abilities were investigated in the following reaction conditions: a solution of DMF and TEOA mixed in the ratio of 5:1 containing the supramolecular photocatalyst and 1-benzyl-1,4-dihydronicotineamide (BNAH; shown in Chart 3) as a sacrificial electron donor were irradiated at λ_{ex} > 500 nm. Only **1** and **6** could work as good photocatalysts for CO_2 reduction.

The UV−vis absorption spectra of the supramolecular photocatalysts **1** and **4**, which differ only in the bridging ligand, are shown with those of the corresponding mononuclear ruthenium(II) and rhenium(I) complexes as two typical examples of the supramolecular photocatalysts (Figure 1). The absorption spectrum of **1** was very similar to the sum spectrum of the corresponding mononuclear complexes (Figure 1a), whereas the spectrum of **4** was slightly different from the sum spectrum of the corresponding model complexes (Figure 1b). These results clearly indicated that each unit in **1** has no strong electronic interaction because of the presence of the alkyl chain between the two diimine moieties in the bridging ligand, whereas there is strong interaction in **4** because of the conjugation in the bridging ligand. Both **1** and **4** selectively photocatalyzed CO_2 reduction and yielded CO; however, their photocatalyses were very different (Figure 2, eq 4). In both cases, only the Ru unit could absorb the irradiated light, and its ^{3}MLCT excited state was reductively quenched, giving the corresponding OERS of the Ru unit in the supramolecular photocatalyst (Scheme 4).

The added electron must be transferred to the Re unit for CO_2 reduction. Moreover, this electron transfer should be faster for **4** than for **1** because of the electronic interaction between the Ru and Re units, which is due to conjugation of

DOI: 10.1021/ic502675a
Inorg. Chem. 2015, 54, 5096−5104

Chart 2. Synthesized Ruthenium(II)−Rhenium(I) Multinuclear Complexes with Various Bridging Ligands[25]

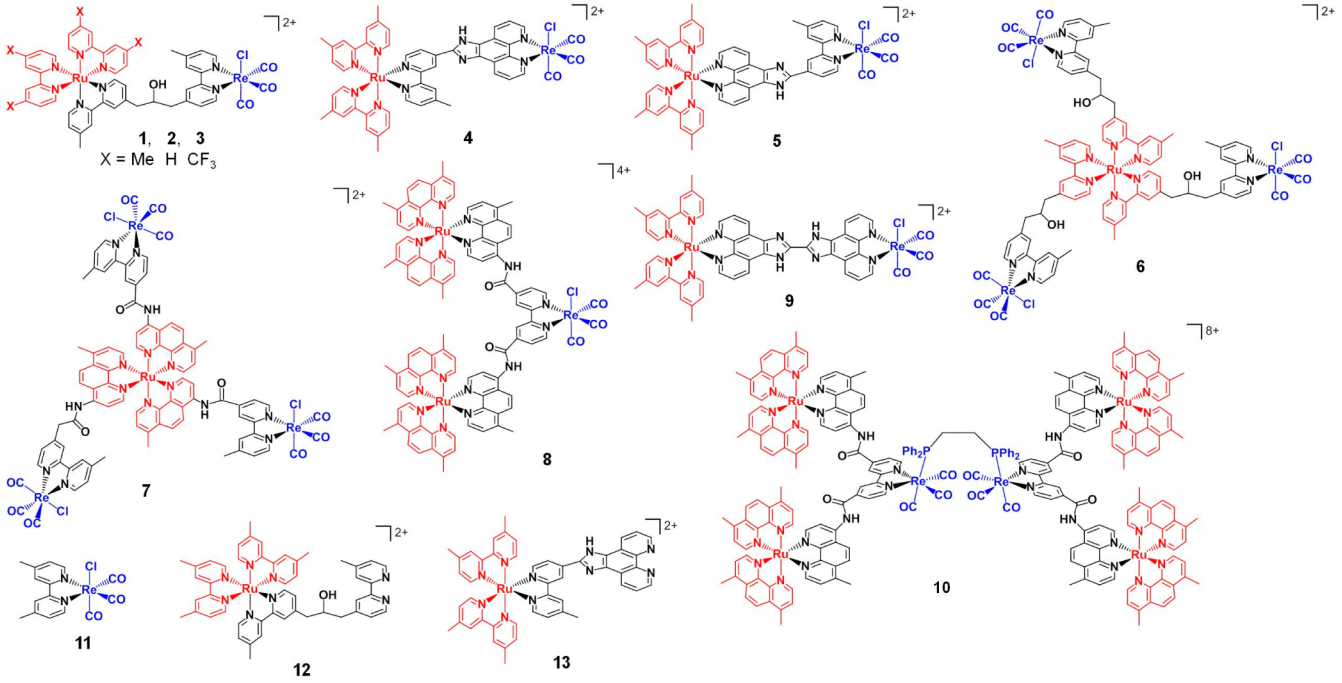

Chart 3. Sacrificial Electron Donors

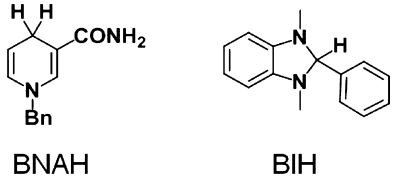

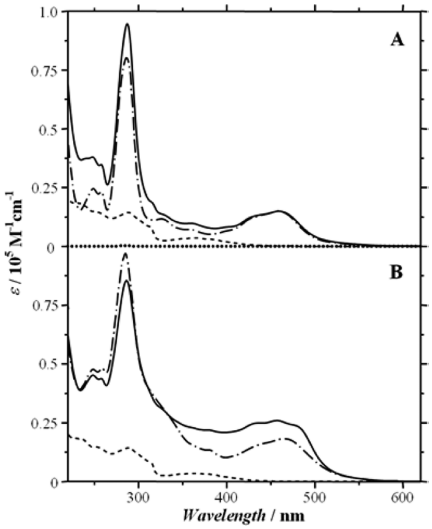

Figure 1. Absorption spectra of metal complexes in MeCN: (A) **11** (dashed line), **12** (dot-dashed line), and **1** (solid line); (B) **13** (dot-dashed line) and **4** (solid line).[25]

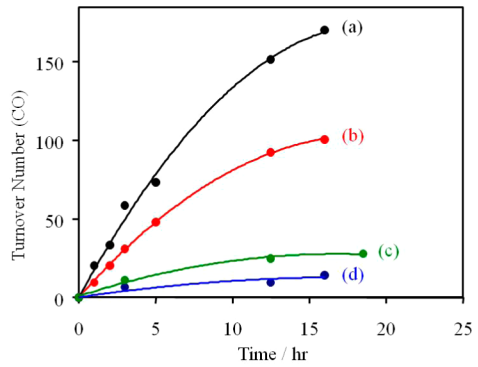

Figure 2. Time course of CO formation during the photocatalytic reduction of CO_2 (λ_{ex} > 500 nm) using (a) **1**, (b) $[Ru(4,4'\text{-}Me_2bpy)_3]^{2+}$ + **11**, (c) **4**, and (d) **5**. The concentration of the complexes was 0.05 mM.[25]

Scheme 4. Reductive Quenching of the ^{3}MLCT Excited State of 1 by BNAH

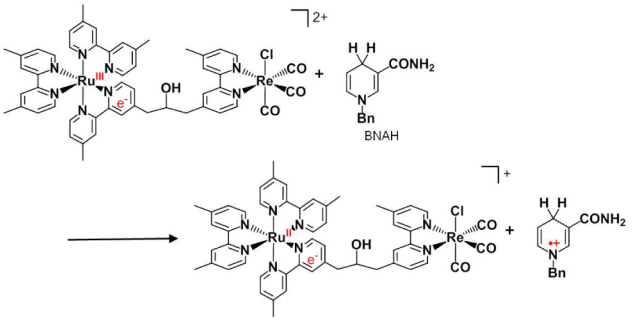

the bridging ligand. However, the turnover number (TON_{CO} = 170) of **1** was much higher than that of the mixed system, i.e., $[Ru(4,4'\text{-}Me_2bpy)_3]^{2+}$ as a photosensitizer and **11** as a catalyst (TON_{CO} = 101, eq 5), and **4** was a much worse photocatalyst compared with the mixed system (TON_{CO} = 28). Table 2 summarizes the reduction potentials of the Ru and Re units and the TON_{CO} of some supramolecular photocatalysts.

$$CO_2 \xrightarrow[\text{BNAH (0.1 M) in DMF−TEOA (5:1, v/v)}]{\textbf{1} \text{ or } \textbf{4}\ (0.05\ \text{mM})/h\nu\ (\lambda_{ex} > 500\ \text{nm})} CO \qquad (4)$$

DOI: 10.1021/ic502675a
Inorg. Chem. 2015, 54, 5096−5104

Table 2. TON_{CO} Values Using Various Supramolecular Photocatalysts and Redox Potentials of Each Unit[25]

		E_{red},[a] V vs $Ag/AgNO_3$	
complex	TON_{CO}	ruthenium	rhenium
1	170	−1.77	−1.77
2	50	−1.73	−1.73
3	3	−1.23	−1.76
4	28	−1.28	−1.10
5	14	−1.10	−1.33
6	240	−1.80	−1.80

[a]A DMF−TEOA (5:1, v/v) solution containing the complex (0.05 mM) and BNAH (0.1 M) was irradiated at λ_{ex} > 500 nm under a CO_2 atmosphere. [b]Measured in MeCN.

$$CO_2 \xrightarrow[\textbf{11}\ (0.05\ mM),\ BNAH\ (0.1\ M)\ in\ DMF-TEOA\ (5:1,\ v/v)]{Ru(4,4'\text{-}Me_2bpy)_3\ (0.05\ mM)/h\nu\ (\lambda_{ex} > 500\ nm)} CO \quad (5)$$

In the cases of **3** and **5**, electron transfer from the OERS of the Ru unit to the Re unit was very slow because the reduction potential of the Ru unit was more positive than that of the Re unit. This is likely the main reason why these two complexes could not work as good photocatalysts for CO_2 reduction. Although in the case of **4** the reduction potential of the Ru unit was more negative than that of the Re unit, photocatalysis of **4** was still low. This problem is caused by the highly positive reduction potential, i.e., very low reduction power of the Re unit. Table 3 summarizes the first reduction potential of various rhenium(I) mononuclear complexes and their photocatalyses for CO_2 reduction.[26]

Table 3. Photocatalytic CO_2 Reduction[a] using Rhenium Mononuclear Complexes and Their Reduction Potentials[26]

$[Re(4,4'\text{-}X_2bpy)(CO)_3(PR_3)]^+$				
X	PR_3	TON_{CO}	Φ_{CO}	E_{red},[b] V
CF_3	$P(OEt)_3$	0.10	0.005	−1.03
H	$P(n\text{-}Bu)_3$	0.65	0.013	−1.39
H	PEt_3	0.83	0.024	−1.39
H	$P(OMe)_3$	5.5	0.17	−1.41
H	$P(OEt)_3$	5.9	0.16	−1.43
H	$P(O\text{-}i\text{-}Pr)_3$	6.2	0.20	−1.44
Me	$P(OEt)_3$	4.1	0.18	−1.55

[a]A 5:1 solution (4 mL) of DMF−TEOA containing a complex (2.6 mM) was irradiated at λ_{ex} = 365 nm. [b]Measured in MeCN. Reference electrode: $Ag/AgNO_3$ (0.1 M).

A drastic change of photocatalysis was observed according to the reduction potentials of the rhenium(I) complexes; i.e., the rhenium(I) complex with a reduction potential more negative than −1.4 V vs $Ag/AgNO_3$ could work as a good photocatalyst, while photocatalyses of complexes with more positive potentials were much lower. The reduction potential of the Re unit in **4** was −1.10 V, much lower than that in **1**, because the conjugation in the bridging ligand lowers the π^*-orbital energy of the diimine moiety in the Re unit. This is probably the main reason why **1** was a much better photocatalyst than **4**. In other words, the alkyl chain between the diimine moieties in the bridging ligand plays the important role of connecting the redox photosensitizer and catalyst but does not lower the π^*-orbital energy of the diimine moiety in the Re unit.

On the basis of the investigations described above, we proposed a molecular architecture for constructing an efficient supramolecular photocatalysts for CO_2 reduction using a ruthenium(II) photosensitizer and a rhenium(I) catalyst:

1. The electron captured by the photosensitizer unit should be mainly localized in the bridging ligand but not in the peripheral ligands of the photosensitizer unit because the electron should transfer to the catalyst unit.
2. However, intramolecular electron transfer as the second step of the photocatalytic reaction is not a rate-limiting process, which should be a process of CO_2 reduction on the catalyst unit, including CO_2 capture on the rhenium center, second-electron insertion to the catalyst unit, and release of CO from the catalyst unit.
3. Conjugation between two diimine moieties in the bridging ligand should not be done because it lowers the reduction power of the catalyst.

According to this molecular architecture, we successfully synthesized various supramolecular photocatalysts for CO_2 reduction with high efficiency (Chart 4 and Table 4). The

Chart 4. Structures of Efficient Supramolecular Photocatalysts for CO_2 Reduction[27−29,35−37]

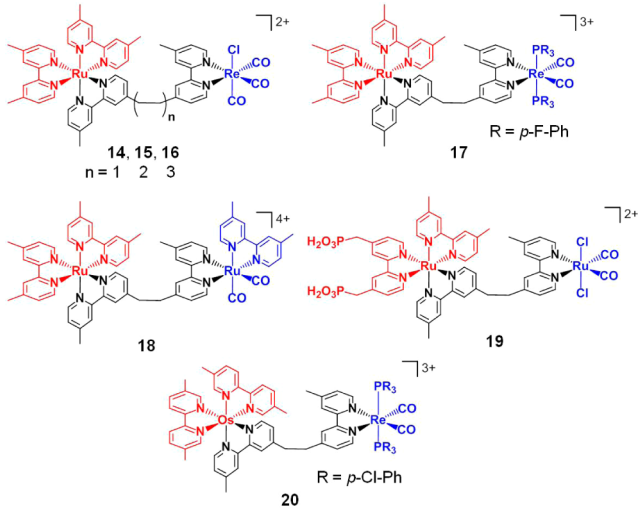

length of the alkyl chain in the bridging ligand affected the activity of CO_2 reduction.[27] The highest photocatalysis (Φ_{CO} and TON_{CO}) was obtained using a ruthenium(II)−rhenium(I) complex containing an ethylene chain ($-CH_2CH_2-$; **14**); on the other hand, when the carbon number of the alkyl chain was 4 (**15**) or 6 (**16**), the photocatalyses of the ruthenium(II)−rhenium(I) complexes were similar. The exceptional behavior of **14** was due to weak electronic interaction between the Ru and Re units through the ethylene chain. The photophysical and electrochemical properties of **14** were slightly different from those of the model ruthenium(II) and rhenium(I) mononuclear complexes containing 4,4′-Me_2bpy as the ligand, while these properties of the other supramolecular photocatalysts were very similar to those of the mononuclear complexes. This weak interaction shifted the oxidation potential of the Ru unit to more positive values, which caused the reductive quenching of the ^{3}MLCT excited state of the Ru unit by BNAH to be more rapid. Although the reduction potential of the Re unit was also slightly shifted to more positive values, it was still much more negative than −1.4 V (E_{red} = −1.72 V vs

DOI: 10.1021/ic502675a
Inorg. Chem. 2015, 54, 5096−5104

Table 4. Photocatalytic CO_2 Reduction Using Supramolecular Photocatalysts[a]

complex	solvent	reductant	TON_{CO}	TON_{HCOOH}	λ_{ex} for TON, nm	Φ_{CO}	Φ_{HCOOH}	λ_{ex} for Φ, nm	intensity,[b] einstein s^{-1}
1	DMF−TEOA (5:1)	BNAH	170		>500	0.12		480	2.6×10^{-8}
14	DMF−TEOA (5:1)	BNAH	180		>500	0.13		546	8.2×10^{-8}
15	DMF−TEOA (5:1)	BNAH	120		>500	0.11		546	8.2×10^{-8}
16	DMF−TEOA (5:1)	BNAH	120		>500	0.11		546	8.2×10^{-8}
17	DMF−TEOA (5:1)	BNAH	207		>500	0.15		480	4.2×10^{-9}
17	DMF−TEOA (5:1)	BIH	3029		>500	0.45		480	4.3×10^{-9}
18	DMF−TEOA (4:1)	BNAH	13	315	>500		0.038	480	4.9×10^{-8}
19	MeOH−TEOA (4:1)	BNAH	5	74	>480				
20	DMF−TEOA (5:1)	BIH	1138	4	>620	0.12		650	1.2×10^{-8}

[a]A 4 mL solution containing 0.05 mM photocatalyst and 0.1 M reductant was irradiated under a CO_2 atmosphere. [b]For quantum efficiency measurement.

Scheme 5. Oxidation and Dimerization Processes of BNAH[29]

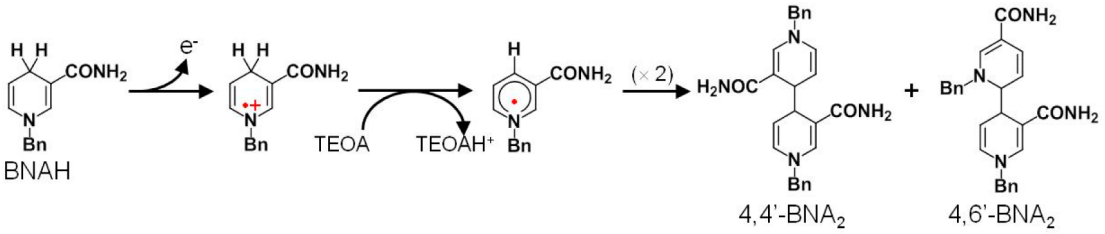

Scheme 6. Oxidation Process of BIH[29]

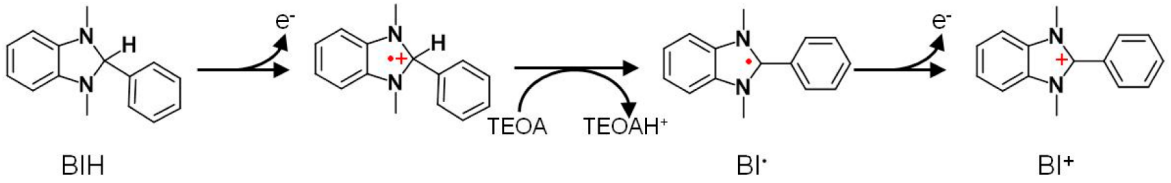

$Ag/AgNO_3$). The effects of the peripheral ligands in the Re unit on the photocatalysis were also investigated. We found that a supramolecular photocatalyst with *cis,trans*-$[Re(N^N)(CO)_2\{P(p\text{-F-Ph})_3\}_2]^+$ as the catalyst unit (**17** in Chart 4) has a very high performance on CO_2 reduction.[28]

For CO_2 reduction using the supramolecular photocatalysts with $[Ru(4,4'\text{-}Me_2bpy)_2(N^N)]^{2+}$-type photosensitizer units, BNAH and 1,3-dimethyl-2-phenyl-2,3-dihydro-1*H*-benzo[*d*]-imidazole (BIH; in Chart 3[29]) were useful reductants, but TEOA was not. This is due to the fact that the former two could reductively quench the ^{3}MLCT excited state of the photosensitizer unit while TEOA could not. However, TEOA was required in the efficient photocatalytic reduction of CO_2 even using BNAH or BIH as the reductant because it worked as a base. Deprotonation from one-electron oxidation products (OEOPs) of BNAH and BIH by TEOA should suppress back electron transfer from the OERS to the OEOP of the supramolecular photocatalyst. Because the BNA radical ($BNA^•$) produced by deprotonation of the OEOP of BNAH rapidly dimerizes to give BNA_2 (Schemes 5 and 6), BNAH functions as a one-electron donor in photocatalytic reactions.[28] On the other hand, BIH worked as a two-electron donor because the radical ($BI^•$) produced by deprotonation from the OEOP of BIH has a much stronger reduction power and a very slow dimerization rate. Because BIH has a stronger reducing power ($E^{ox}_{1/2}$ = 0.33 V vs SCE[30]) than BNAH (E^{oox} = 0.57 V vs SCE[31]), BIH could quantitatively quench the excited state of $[Ru(4,4'\text{-}Me_2bpy)_3]^{2+}$,[29] while the quenching by BNAH was only 49%.[28] For these reasons, the usage of BIH ensured a better performance of the supramolecular photocatalysts compared with BNAH. To our knowledge, photocatalysis of **17** using BIH (Φ_{CO} = 0.45, TON_{CO} = 3029, and TOF_{CO} = 35.7 min^{-1}) is the highest among those of the reported supramolecular photocatalysts.[29]

The proposed molecular architecture could be applied to the synthesis of various types of supramolecular photocatalysts. If the $[Ru(N^N)_2(CO)_2]^{2+}$[32,33] and *cis,trans*-$Ru(N^N)(CO)_2Cl_2$[34] types were used as the catalyst units instead of the Re catalyst unit (**18**[35] and **19**[36] in Chart 4, respectively), the main photocatalytic reduction product of CO_2 was HCOOH (Figure 3 shows the result in the case of **18**). The mixed system of the corresponding mononuclear photosensitizer and catalyst showed much lower activity because of the formation of ruthenium(0) polymers containing Ru−Ru bonds.[35] The supramolecular photocatalyst with one photosensitizer unit and one catalyst unit, on the other hand, was not converted to such polymers probably because of the steric hindrance of the photosensitizer unit.

The photosensitizer unit could also be changed to a different metal complex. To utilize a wider range of visible light, $[Os(5,5'\text{-}Me_2bpy)_2(N^N)]^{2+}$ was used as the photosensitizer unit instead of the ruthenium(II) complex (**20** in Chart 4). The osmium(II) complex absorbs light at a wavelength longer by about 200 nm than the corresponding ruthenium complex because of relatively strong S−T absorption band (Figure 4).[37] Irradiation at λ_{ex} > 620 nm to a DMF−TEOA solution containing **20** and BIH under a CO_2 atmosphere induced photocatalytic CO formation (Φ_{CO} = 0.12 and TON_{CO} =

DOI: 10.1021/ic502675a
Inorg. Chem. 2015, 54, 5096−5104

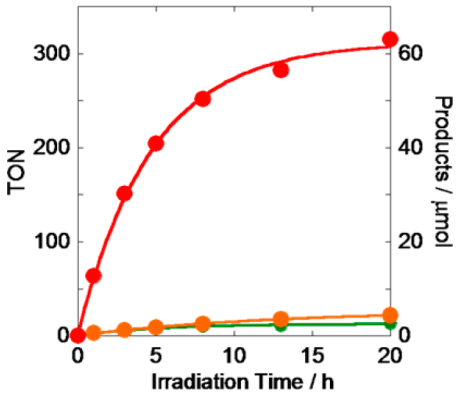

Figure 3. Photocatalytic formation of formic acid (red), CO (green), and H_2 (orange) as a function of the irradiation time: A CO_2-saturated DMF−TEOA (4:1, v/v; 4 mL) solution containing BNAH (0.1 M) and **18** (0.05 mM) was irradiated at λ_{ex} > 500 nm.[35]

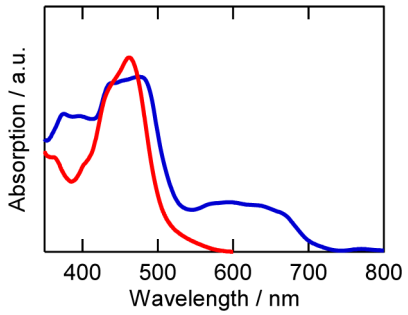

Figure 4. UV−vis absorption spectra of $[Os(5,5'\text{-}Me_2bpy)_2(4,4'\text{-}Me_2bpy)]^{2+}$ (blue) and $[Ru(4,4'\text{-}Me_2bpy)_3]^{2+}$ (red).[37]

1138), while no photoreduction product of CO_2 was observed using **17** instead of **20** because **17** does not absorb at λ > 620 nm.

HYBRID PHOTOCATALYST WITH A SEMICONDUCTOR

Although we have successfully developed supramolecular photocatalysts that can drive efficient photocatalytic CO_2 reduction as described above, an electron donor with a strong reduction power such as BNAH and BIH is required because the oxidation power of the ruthenium photosensitizer unit is relatively weak. It is necessary to strengthen the oxidation power and finally use water as the electron donor to allow these efficient photocatalytic systems to perform a useful artificial photosynthesis.

Recently, many visible-light-driven semiconductor photocatalysts have been reported for photocatalytic water oxidation to produce O_2.[38−41] However, they are generally inferior to the metal complex photocatalysts for CO_2 reduction because their photocatalysis has low selectivity owing to the competing production of H_2.[42−44] If we could hybridize a metal complex photocatalyst for CO_2 reduction and a semiconductor photocatalyst with strong oxidation power, a novel type of photocatalytic system for CO_2 reduction with water as the reductant might be developed. From this viewpoint, the supramolecular photocatalysts have advantageous structures. If both the redox photosensitizer and catalyst in the two-component system are fixed on the surface of a semiconductor photocatalyst, collision between the OERS of the photosensitizer and the catalyst should be a very slow or impossible process. We do not need to worry about this when the supramolecular photocatalyst is adsorbed on the semiconductor surface because the two components are already connected to each other. Additionally, if anchor groups, which are connected on the surface of the semiconductor, are introduced into the photosensitizer unit, the rapid intramolecular electron transfer might suppress the problematic back electron transfer from the OERS of the photosensitizer unit to the semiconductor because of the longer distance between the catalyst and semiconductor. To construct hybrid systems with supramolecular and semiconductor photocatalysts, we can consider two strategies. The first one is the direct immobilization of the metal complex to a powdered semiconductor photocatalyst. Both of them should sequentially absorb photons to achieve both strong reduction and oxidation powers, respectively, i.e., the so-called Z-Scheme process.

In this case, a photochemically produced electron in the conduction band (and/or defect level) of the semiconductor transfers to the excited state of the photosensitizer unit of the supramolecular photocatalyst. The second strategy is the usage of a semiconductor photoanode and a supramolecular photocatalyst adsorbed on a photocathode such as a p-type semiconductor electrode. A photochemically generated electron on the photoanode should be transferred to the excited state of the photosensitizer unit of the supramolecular photocatalyst from the cathode via a wire connecting both electrodes. Either way, both the supramolecular photocatalyst and the semiconductor should absorb photons step by step to achieve both an added electron in the catalyst unit of the supramolecular photocatalyst, which has strong reduction power, and a hole in the valence band of the semiconductor, which has strong oxidation power.

We recently reported on the former type of hybrid, which was a powder-type artificial Z-Scheme photocatalyst; i.e., a supramolecular photocatalyst (**19**) with a *cis,trans*-Ru(N^N)-$(CO)_2Cl_2$ moiety as the catalyst for CO_2 reduction and a $[Ru(4,4'\text{-}Me_2bpy)(N^N)\{4,4'\text{-}(H_2O_3PCH_2)_2bpy\}]^{2+}$ photosensitizer having methylphosphonate groups as anchors to metal oxides were adsorbed on tantalum oxynitride powders with silver nanosized particles on the surface (Ag/TaON).[36] This hybrid **19**−Ag/TaON was dispersed in methanol and irradiated by visible light (λ_{ex} > 400 nm) under a CO_2 atmosphere to give HCOOH as the main reduction product with CO and H_2. HCHO was also detected, of which the produced amount was similar to the sum of the reductive products. In the case of using $^{13}CH_3OH$ as the solvent, only $H^{13}CHO$ was observed in the gas chromatography (GC)/mass spectrometry (MS) analysis of the photocatalytic reaction solution (Figure 5c,d). These results show that the electron source of the reduction products was methanol. Using $^{13}CO_2$, the carbon source of HCOOH was also clarified to be CO_2 (Figure 5a,b). Photocatalytic reduction of CO_2 did not proceed using the supramolecular photocatalyst without Ag/TaON (Table 5) because the excited state of the photosensitizer unit could not oxidize methanol. Although irradiation to a suspension of Ag/TaON without the supramolecular photocatalyst under a CO_2 atmosphere catalytically produced H_2, no reduction product of CO_2 was observed. In the case of using Ag/TaON adsorbed with only the ruthenium mononuclear complexes as the catalyst model, i.e., *cis,trans*-Ru$\{4,4'\text{-}(H_2O_3PCH_2)_2bpy\}(CO)_2Cl_2$ (**21**), instead of **19**−Ag/TaON, very small amounts of HCOOH (TON_{HCOOH} = 0.8) and CO (TON_{CO} = 0.9) were produced with a considerable amount of

DOI: 10.1021/ic502675a
Inorg. Chem. 2015, 54, 5096−5104

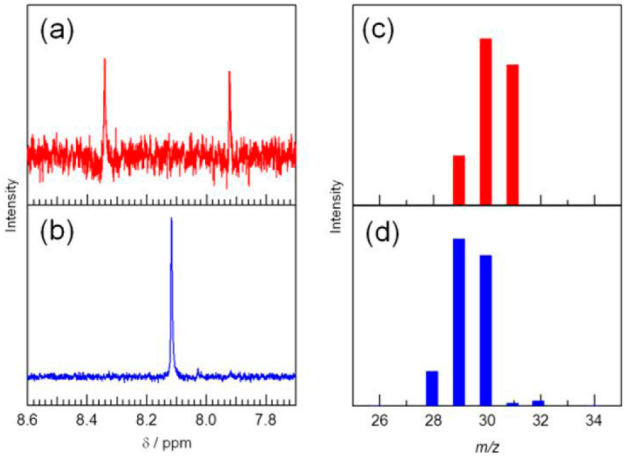

Figure 5. ^{1}H NMR spectra of the photocatalytic reaction solutions (4 mL): **19**−Ag/TaON (8 mg) was irradiated at λ_{ex} > 400 nm for 15 h in (a) CH_3OH under $^{13}CO_2$ (670 Torr) and (b) CH_3OH saturated with unlabeled CO_2. MS spectra of formaldehyde peaks in the GC/MS analysis of the photocatalytic reaction solutions: **19**−Ag/TaON (1 mg) was irradiated at λ_{ex} > 400 nm for 24 h in (c) unlabeled CO_2-saturated $^{13}CH_3OH$ (0.2 mL) and (d) unlabeled CH_3OH (0.2 mL). Adapted with permission from ref 36. Copyright 2012 American Chemical Society.

H_2. Even using **19**−Ag/TaON, neither the CO_2 reduction products nor H_2 was produced without irradiation. These results clearly indicate that the reaction proceeds via step-by-step absorption of two photons by both Ag/TaON and **19**, i.e., through an artificial Z-Scheme mechanism. The photocatalytic reaction was probably initiated by photooxidation of methanol with a hole in the valence band of the excited Ag/TaON, followed by electron transfer from the Ag/TaON to the ^{3}MLCT excited state of the photosensitizer unit of **19**. Without the silver nanoparticles on TaON, photocatalysis of the hybrid for both CO_2 reduction and H_2 production was much lower than that with silver. The silver nanoparticles assist the photochemical charge separation in TaON because the photocatalytic H_2 evolution of TaON was accelerated by the deposition of silver. Other possible roles of the deposited silver are to serve as an electron pool located closely to the supramolecular photocatalysts and as an energy source via plasmon excitation of the nanosized silver particles of which the excitation band was observed in the UV−vis diffraction spectrum of **19**−Ag/TaON. Verifications of these roles are now in progress in our laboratory.

In conclusion of this section, we successfully developed a novel type of artificial Z-Scheme photocatalyst (i.e., **19**−Ag/TaON) for CO_2 reduction, of which photocatalysis is revealed by stepwise excitation of both the Ag/TaON and **19** units, followed by oxidation of methanol on the former unit and reduction of CO_2 on the latter unit. This photocatalytic reaction, which is shown in eq 6, is an endergonic reaction by ΔG° = +83.0 kJ mol^{-1}, which indicates that visible-light energy can be converted into chemical energy using this photocatalyst.

$$CO_2 + CH_3OH \rightarrow HCOOH + HCHO \qquad \Delta G^\circ = +83.0\ \text{kJ mol}^{-1} \tag{6}$$

In the artificial Z-Scheme photocatalyst, the supramolecular photocatalyst plays crucial roles such as inducing efficient electron transfer from the OERS of the photosensitizer unit to the catalyst unit because the two units are connected to each other and depleting back electron transfer from the OERS of the photosensitizer unit to Ag/TaON because of rapid electron transfer to the catalyst unit.

CONCLUSION

We reviewed our recent progress in photocatalysts for CO_2 reduction. These studies clearly show that highly efficient photocatalysis can be achieved using metal complexes as a redox photosensitizer and catalyst. The supramolecular photocatalysts, in which the photosensitizer and catalyst were connected to each other via a bridging ligand, have more efficient and durable photocatalyses compared with the corresponding mixtures of the mononuclear photosensitizer and catalyst. Supramolecular photocatalysts have another advantage when the molecular photocatalytic systems are adsorbed on the solid surface because electron transfer from the photosensitizer unit to the catalyst unit can smoothly proceed even on the surface. In addition, we demonstrated this in the case of the hybrid photocatalyst with a semiconductor. This system is the first example of a visible-light-driven photocatalyst for CO_2 reduction via the Z-Scheme mechanism, where the semiconductor and the photosensitizer unit of the supramolecular photocatalyst are excited step-by-step in order to transfer an electron from the semiconductor to the catalyst unit.

The next steps in the field of photocatalytic reduction of CO_2 should be the addition of the various functions to the photocatalytic systems such as light-harvesting, collection of CO_2 for using a low concentration of CO_2, and water oxidation. These studies are in progress.

AUTHOR INFORMATION

Corresponding Author

*E-mail: ishitani@chem.titech.ac.jp.

Notes

The authors declare no competing financial interest.

Table 5. Products after 15 h of Irradiation under Various Photocatalytic Reaction Conditions[a]

photocatalyst	metal complex, nmol	irradiation	HCOOH, nmol (TON_{HCOOH})[b]	H_2, nmol	CO, nmol (TON_{CO})[b]
19−Ag/TaON	24	on	969 (41)	678	68 (2.8)
19[c]	24	on	35 (1.5)	90	40 (1.8)
Ag/TaON	0	on	n.d.	480	n.d.
21−Ag/TaON[d]	25	on	19 (0.8)	437	23 (0.9)
19−Ag/TaON	25	off	n.d.	10	n.d.
19−TaON	22	on	69 (3.1)	170	15 (0.7)

[a]Photocatalyst (8 mg) was dispersed in 4 mL of methanol. Reaction conditions: CO_2 bubbling for 20 min before irradiation using a 500 W mercury lamp with a cutoff filter (λ_{ex} > 400 nm). [b]TONs were calculated on the basis of the metal complex used. [c]**19** (6 μM) in a methanol solution. [d]**21** is *cis,trans*-Ru{4,4′-$(H_2O_3PCH_2)_2$bpy}$(CO)_2Cl_2$.

DOI: 10.1021/ic502675a
Inorg. Chem. 2015, 54, 5096−5104

■ ACKNOWLEDGMENTS

This work was partially supported by a Grant-in-Aid for Scientific Research on Innovative Areas "Artificial photosynthesis (AnApple)" (Grant 24107005) from the Japan Society for the Promotion of Science.

■ REFERENCES

(1) BP statistical Review of World Energy 2014, Christof Rühl, June 2014, http://www.bp.com/en/global/corporate/about-bp/energy-economics/statistical-review-of-world-energy.html.
(2) Roy, S. C.; Varghese, O. K.; Paulose, M.; Grimes, C. A. *ACS Nano* **2010**, *4*, 1259−1278.
(3) Berardi, S.; Drouet, S.; Francàs, L.; Gimbert-Suriñach, C.; Guttentag, M.; Richmond, C.; Stoll, T.; Llobet, A. *Chem. Soc. Rev.* **2014**, *43*, 7501−7519.
(4) Knör, G. *Coord. Chem. Rev.* **2014**, in press.
(5) Tanaka, K.; Ooyama, D. *Coord. Chem. Rev.* **2002**, *226*, 211−218.
(6) Lehn, J.-M.; Ziessel, R. *Proc. Natl. Acad. Sci. U.S.A.* **1982**, *79*, 701−704.
(7) Kumar, B.; Smieja, J. M.; Kubiak, C. P. *J. Phys. Chem. C* **2010**, *114*, 14220−14223.
(8) Kumar, B.; Smieja, J. M.; Sasayama, A. F.; Kubiak, C. P. *Chem. Commun.* **2012**, *48*, 272−274.
(9) Bruckmeier, C.; Lehenmeier, M. W.; Reithmeier, R.; Rieger, B.; Herranz, J.; Kavakli, C. *Dalton Trans.* **2012**, *41*, 5026−5037.
(10) Portenkirchner, E.; Oppelt, K.; Ulbricht, C.; Egbe, D. A. M.; Neugebauer, H.; Knör, G.; Sariciftci, N. S. *J. Organomet. Chem.* **2012**, *716*, 19−25.
(11) Hawecker, J.; Lehn, J.-M.; Ziessel, R. *J. Chem. Soc., Chem. Commun.* **1983**, 536−538.
(12) Hawecker, J.; Lehn, J.-M.; Ziessel, R. *Helv. Chim. Acta* **1986**, *69*, 1990−2012.
(13) Kutal, C.; Weber, M. A.; Ferraudi, G.; Geiger, D. *Organometallics* **1985**, *4*, 2161−2166.
(14) Kalyanasundaram, K. *J. Chem. Soc., Faraday Trans. 2* **1986**, *82*, 2401−2415.
(15) Kutal, C.; Corbin, J. A.; Ferraudi, G. *Organometallics* **1987**, *6*, 553−557.
(16) Hayashi, Y.; Kita, S.; Brunschwig, B. S.; Fujita, E. *J. Am. Chem. Soc.* **2003**, *125*, 11976−11987.
(17) Takeda, H.; Koike, K.; Inoue, H.; Ishitani, O. *J. Am. Chem. Soc.* **2008**, *130*, 2023−2031.
(18) Morimoto, T.; Nakajima, T.; Sawa, S.; Nakanishi, R.; Imori, D.; Ishitani, O. *J. Am. Chem. Soc.* **2013**, *135*, 16825−16828.
(19) Morimoto, T.; Nishiura, C.; Tanaka, M.; Rohacova, J.; Nakagawa, Y.; Funada, Y.; Koike, K.; Yamamoto, Y.; Shishido, S.; Kojima, T.; Saeki, T.; Ozeki, T.; Ishitani, O. *J. Am. Chem. Soc.* **2013**, *135*, 13266−13269.
(20) Thoi, V. S.; Kornienko, N.; Margarit, C. G.; Yang, P.; Chang, C. J. *J. Am. Chem. Soc.* **2013**, *135*, 14413−14424.
(21) Kuramochi, Y.; Kamiya, M.; Ishida, H. *Inorg. Chem.* **2014**, *53*, 3326−3332.
(22) Kimura, E.; Bu, X.; Shionoya, M.; Wada, S.; Maruyama, S. *Inorg. Chem.* **1992**, *31*, 4542−4546.
(23) Kimura, E.; Wada, S.; Shionoya, M.; Okazaki, Y. *Inorg. Chem.* **1994**, *33*, 770−771.
(24) Komatsuzaki, N.; Himeda, Y.; Hirose, T.; Sugihara, H.; Kasuga, K. *Bull. Chem. Soc. Jpn.* **1999**, *72*, 725−731.
(25) Gholamkhass, B.; Mametsuka, H.; Koike, K.; Tanabe, T.; Furue, M.; Ishitani, O. *Inorg. Chem.* **2005**, *44*, 2326−2336.
(26) Koike, K.; Hori, H.; Ishizuka, M.; Westwell, J. R.; Takeuchi, K.; Ibusuki, T.; Enjouji, K.; Konno, H.; Sakamoto, K.; Ishitani, O. *Organometallics* **1997**, *16*, 5724−5729.
(27) Koike, K.; Naito, S.; Sato, S.; Tamaki, Y.; Ishitani, O. *J. Photochem. Photobiol. A: Chem.* **2009**, *207*, 109−114.
(28) Tamaki, Y.; Watanabe, K.; Koike, K.; Inoue, H.; Morimoto, T.; Ishitani, O. *Faraday Discuss.* **2012**, *155*, 115−127.
(29) Tamaki, Y.; Koike, K.; Morimoto, T.; Ishitani, O. *J. Catal.* **2013**, *304*, 22−28.
(30) Hasegawa, E.; Takizawa, S.; Seida, T.; Yamaguchi, A.; Yamaguchi, N.; Chiba, N.; Takahashi, T.; Ikdeda, H.; Akiyama, K. *Tetrahedron* **2006**, *62*, 6581−6588.
(31) Fukuzumi, S.; Koumitsu, S.; Hironaka, K.; Tanaka, T. *J. Am. Chem. Soc.* **1987**, *109*, 305−316.
(32) Ishida, H.; Tanaka, K.; Tanaka, T. *Organometallics* **1987**, *6*, 181−186.
(33) Ishida, H.; Terada, T.; Tanaka, K.; Tanaka, T. *Inorg. Chem.* **1990**, *29*, 905−911.
(34) Ishida, H.; Fujiki, K.; Ohba, T.; Ohkubo, K.; Tanaka, K.; Terada, T.; Tanaka, T. *J. Chem. Soc., Dalton Trans.* **1990**, 2155−2160.
(35) Tamaki, Y.; Morimoto, T.; Koike, K.; Ishitani, O. *Proc. Natl. Acad. Sci. U. S. A.* **2012**, *109*, 15673−15678.
(36) Sekizawa, K.; Maeda, K.; Domen, K.; Koike, K.; Ishitani, O. *J. Am. Chem. Soc.* **2013**, *135*, 4596−4599.
(37) Tamaki, Y.; Koike, K.; Morimoto, T.; Yamazaki, Y.; Ishitani, O. *Inorg. Chem.* **2013**, *52*, 11902−11909.
(38) Hitoki, G.; Takata, T.; Kondo, J. N.; Hara, M.; Kobayashi, H.; Domen, K. *Chem. Commun.* **2002**, 1698−1699.
(39) Zhang, F.; Yamakata, A.; Maeda, K.; Moriya, Y.; Takata, T.; Kubota, J.; Teshima, K.; Oishi, S.; Domen, K. *J. Am. Chem. Soc.* **2012**, *134*, 8348−8351.
(40) Kudo, A.; Omori, K.; Kato, H. *J. Am. Chem. Soc.* **1999**, *121*, 11459−11467.
(41) Ma, S. S. K.; Maeda, K.; Abe, R.; Domen, K. *Energy Environ. Sci.* **2012**, *5*, 8390−8397.
(42) Yui, T.; Kan, A.; Saitoh, C.; Koike, K.; Ibusuki, T.; Ishitani, O. *ACS Appl. Mater. Interfaces* **2011**, *3*, 2594−2600.
(43) Iizuka, K.; Wato, T.; Miseki, Y.; Saito, K.; Kudo, A. *J. Am. Chem. Soc.* **2011**, *133*, 20863−20868.
(44) Teramura, K.; Iguchi, S.; Mizuno, Y.; Shishido, T.; Tanaka, T. *Angew. Chem., Int. Ed.* **2012**, *51*, 8008−8011.

DOI: 10.1021/ic502675a
Inorg. Chem. 2015, 54, 5096−5104